Published OnlineFirst August 3, 2010; DOI: 10.1158/1535-7163.MCT-10-0262
Published OnlineFirst on August 3, 2010 as 10.1158/1535-7163.MCT-10-0262

Molecular Cancer Therapeutics

Galectin-3 Promotes Chronic Activation of K-Ras and Differentiation Block in Malignant Thyroid Carcinomas

Ran Levy[1], Meital Grafi-Cohen[2], Zaki Kraiem[3], and Yoel Kloog[1]

Abstract

Anaplastic thyroid carcinomas are deadly tumors that are highly invasive, particularly into the bones. Although oncogenic Ras can transform thyroid cells into a severely malignant phenotype, thyroid carcinomas do not usually harbor *ras* gene mutations. Therefore, it is not known whether chronically active Ras contributes to thyroid carcinoma cell proliferation, although galectin-3 (Gal-3), which is strongly expressed in thyroid carcinomas but not in benign tumors or normal glands, is known to act as a K-Ras chaperone that stabilizes and drives K-Ras.GTP nanoclustering and signal robustness. Here, we examined the possibility that thyroid carcinomas expressing high levels of Gal-3 exhibit chronically active K-Ras. Using cell lines representing three types of malignant thyroid tumors—papillary, follicular, and anaplastic—we investigated the possible correlation between Gal-3 expression and active Ras content, and then examined the therapeutic potential of the Ras inhibitor S-trans, *trans*-farnesylthiosalicylic acid (FTS; Salirasib) for thyroid carcinoma. Thyroid carcinoma cells strongly expressing Gal-3 showed high levels of K-Ras.GTP expression, and K-Ras.GTP transmitted strong signals to extracellular signal-regulated kinase. FTS disrupted interactions between Gal-3 and K.Ras, strongly reduced K-Ras.GTP and phospho-extracellular signal-regulated kinase expression, and enhanced the expression of the cell cycle inhibitor p21 as well as of the thyroid transcription factor 1, which is involved in thyroid cell differentiation. FTS also inhibited anaplastic thyroid carcinoma cell proliferation *in vitro* and tumor growth in nude mice. We conclude that wild-type K-Ras.GTP in association with Gal-3 contributes to thyroid carcinoma malignancy and that Ras inhibition might be a useful treatment strategy against these deadly tumors. *Mol Cancer Ther; 9(8); 2208–19. ©2010 AACR.*

Introduction

More than 95% of thyroid carcinomas are derived from follicular cells, whereas a minority of thyroid tumors (3%) are medullary in origin (1). Most of the carcinomas derived from follicular epithelial cells are indolent tumors that can be effectively managed by surgical resection with or without radioactive iodine ablation. However, a subset of these tumors can behave aggressively, and there is currently no effective form of treatment (2).

Follicular thyroid carcinomas comprise a broad spectrum of tumors that range, on the basis of histologic and clinical parameters, from well-differentiated to undifferentiated types (3). Well-differentiated types include papillary and follicular thyroid carcinomas for which the prognosis is generally good, in contrast to the undifferentiated anaplastic thyroid carcinomas, which are extremely aggressive and usually lethal (4). Anaplastic thyroid carcinomas are characterized by high cellular proliferation rates, increased vascularization, and focal necrosis, which result in a neck mass that enlarges rapidly, invading adjacent tissues and metastasizing particularly into bones. No effective treatment is available and death usually occurs within 1 year of diagnosis (5). Surgery, chemotherapy, and radiotherapy are the conventional therapeutic strategies used in an attempt to improve survival. In many patients, surgery is not feasible, with operability varying from 17% to 65% across reported series (6). Due to the aggressive character of these tumors and their potential for systemic spread, many different chemotherapy regimens have been tried, including doxorubicin, which has shown at best a 22% partial response rate.

Characterization of thyroid carcinomas is based *inter alia* on molecular markers (7). Several important markers for thyroid carcinomas have been described. One of these is galectin-3 (Gal-3), which acts extracellularly as a β-galactoside–binding protein (8) and intracellularly as a scaffold of the K-Ras protein (9–11). Ras proteins act as binary switches alternating between guanosine diphosphate-bound (inactive) and guanosine triphosphate-bound (active) states (12). They activate a multitude of effectors including Raf, phosphatidylinositol-3-OH kinase (PI3-K), and Ral-guanine nucleotide exchange factors), which together regulate cell proliferation, differentiation, survival, and death (13).

Authors' Affiliations: [1]Department of Neurobiology, The George S. Wise Faculty of Life Sciences, Tel Aviv University and [2]Institute of Endocrinology, Metabolism and Hypertension, The Tel Aviv Sourasky Medical Center, Tel Aviv, Israel; and [3]The Ruth and Bruce Rappaport Faculty of Medicine, Technion-Israel Institute of Technology, Haifa, Israel

Corresponding Author: Yoel Kloog, Department of Neurobiology, The George S. Wise Faculty of Life Sciences, Tel Aviv University, 69978 Tel-Aviv, Israel. Phone: 972-3-640-9699; Fax: 972-3-640-7643. E-mail: kloog@post.tau.ac.il

doi: 10.1158/1535-7163.MCT-10-0262

Published OnlineFirst August 3, 2010; DOI: 10.1158/1535-7163.MCT-10-0262

Ras proteins also play a major role in human malignancies. Approximately 30% of all human tumors express oncogenic Ras proteins that are constitutively active and contribute to tumorigenesis, tumor maintenance, invasion, and progression (14). The most prevalent oncogenic *ras* mutations are detected in the *K-ras* gene in pancreatic, colon, and lung cancers (15). The frequency of *ras* gene mutations in thyroid cancer varies with the type of tumor, ranging from 21% to 60% (1). Other factors that can contribute to Ras activation in thyroid tumors include hyperactive tyrosine kinase growth factor receptors (16) and the expression of Ras scaffold proteins that may lead to chronic activation of Ras (9, 17). Among the most common aberrations in thyroid tumors are chimeras of the epidermal growth factor receptor, which are constitutively active and act upstream of Ras especially in papillary thyroid carcinoma (18), and B-Raf mutations leading to constitutive activation of mitogen-activated protein/extracellular signal-regulated kinase (ERK) kinase (MEK) and ERK (19).

Our group has previously shown that Gal-3 acts as a selective intracellular scaffold of K-Ras.GTP in the plasma membrane and enhances Ras signaling (9). More recently, we found that Gal-3 acts as the driving force for K-Ras nanoclustering and signal robustness (11). We showed that Gal-3 overexpression in cancer cells, which increases K-Ras signal output, represents an oncogenic subversion of K-Ras.GTP nanoclusters in the plasma membrane. An important finding was that relatively high expression levels of Gal-3 can be detected in thyroid carcinomas, whereas relatively low levels of Gal-3 are detected in benign tumors or normal glands (20, 21). Accordingly, we postulated that overexpression of Gal-3 contributes to both an increase in K-Ras.GTP and Ras signaling in malignant thyroid carcinomas. If this is shown to be the case, Ras inhibitors might be considered as a potential targeted therapy for highly malignant thyroid carcinomas. Here, we examined this possibility using cell lines that represent three types of malignant tumors of the thyroid gland: papillary (NPA cell line), follicular (WRO and MRO cell lines), and anaplastic (ARO cell line). We first sought a possible correlation between expression levels of Gal-3 and active Ras. We then examined the potential use of the Ras inhibitor S-trans, *trans*-farnesylthiosalicylic acid (FTS; Salirasib) as a therapeutic agent for the treatment of thyroid carcinoma. Our results indicated that cells that strongly express Gal-3 are significantly associated with high expression levels Ras.GTP and K-Ras.GTP, and are highly sensitive to FTS.

Materials and Methods

Cell lines and reagents

Four well-established and extensively studied human thyroid carcinoma cell lines, namely ARO 81-1 (anaplastic), MRO 87-1 and WRO 82-1 (follicular), and NPA (papillary), were kindly provided by Dr. G.J.F. Juillard (University of California at Los Angeles, Los Angeles, CA). The medullar thyroid carcinoma cell line TT was obtained from American Type Culture Collection. The presence of the thyroid-specific transcription factors TTF-1 and PAX-8 in these cell lines confirmed their thyroid origin. Benign human thyroid cells (N465, P473, and D499) were obtained at thyroid dichotomy from tissues of patients with benign colloid nodules (22, 23). All cell lines were cultured (4×10^5 cells per 10-cm plate for 48 h in RPMI containing 10% FCS, 2 mmol/L L-glutamine, 100 U/mL penicillin, and 100 g/mL streptomycin). The cells were incubated at 37°C in a humidified atmosphere with 5% CO_2.

FTS was a gift from Concordia Pharmaceuticals. An enhanced chemiluminescence (ECL) kit was purchased from Amersham Pharmacia Biotech; Hoechst 33258 was purchased from Sigma-Aldrich; and U0126 and LY-294 were purchased from AG Scientific. Mouse anti-pan-Ras (Ab-3), mouse anti–N-Ras, and mouse anti–K-Ras antibodies (Ab) were obtained from Calbiochem; rabbit anti-p21, rabbit anti–TTF-1, and rabbit anti–β-tubulin Abs were from Santa Cruz Biotechnology; mouse anti–phospho-ERK Ab was from Sigma-Aldrich; rabbit anti–phospho-Akt (ser473) and rabbit anti–glyceraldehyde-3-phosphate dehydrogenase (14C10) Abs were from Cell Signaling Technology. Peroxidase-conjugated goat anti-mouse IgG, peroxidase-conjugated goat anti-rat IgG, and peroxidase-conjugated goat anti-rabbit IgG were from Jackson ImmunoResearch Laboratories.

Protein bands were quantified by densitometry with the Image EZQuant-Gel software (EZQuant Ltd.).

Transfection assays

For transfection assays, 2×10^5 ARO cells per well and the same number of MRO cells per well were plated in six-well plates. On the following day, the cells were transfected with plasmid DNA coding for green fluorescent protein (GFP)-Ras(17N) (2 μg) or with a vector with control coding for GFP (2 μg), using a Lipofectamine 2000 transfection kit (Invitrogen).

Cell proliferation assay

ARO, MRO, and NPA cells were plated in 5% FCS media at a density of 1.5×10^4 cells per well in 96-well plates. On the following day, cells were treated with 50, 75, or 100 μmol/L FTS or the vehicle (0.1% DMSO). Proliferation was assessed by incorporation of bromodeoxyuridine (BrdUrd), using the BrdUrd cell proliferation assay kit (Calbiochem).

Cell viability

ARO, MRO, and NPA cells (all at 1.5×10^4 cells/well in 96-well plates) were treated for 24 hours with 50, 75, or 100 μmol/L FTS or the vehicle (0.1% DMSO). Cell viability was estimated by the alamarBlue assay (Serotec) according to the manufacturer's instructions.

Western immunoblotting

ARO, MRO, and NPA (0.4×10^6 cells/10-cm) were cultured in RPMI 1640 containing 5% FCS. Cells were treated with 75 μmol/L FTS or with the vehicle (0.1%

Published OnlineFirst August 3, 2010; DOI: 10.1158/1535-7163.MCT-10-0262

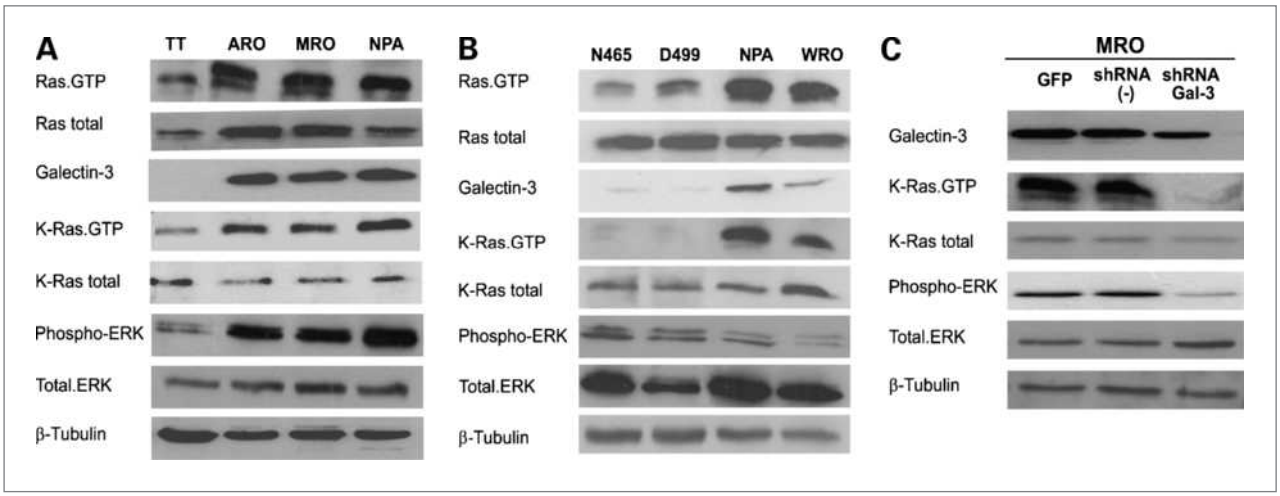

Figure 1. Gal-3 expression in thyroid carcinoma cells correlates positively with the expression of K-Ras.GTP. Cells of the medullary thyroid carcinoma cell line TT and of the thyroid carcinoma cell lines ARO, NPA, MRO, and WRO were homogenized, and expression levels of Ras.GTP, Ras total, Gal-3, K-Ras.GTP, K-Ras total, and the Ras downstream effector ERK and phospho-ERK were determined in aliquots of the cell homogenates by SDS-PAGE followed by immunoblotting with the relevant specific Abs as described in Materials and Methods. β-Tubulin served as a loading control. Shown are typical immunoblots visualized by ECL. A, thyroid carcinoma cell lines. B, benign human thyroid and thyroid carcinoma WRO and NPA cell lines. The NPA cell line served as a positive control. C, MRO cells were infected with retroviruses containing distinct shRNA sequence against Gal-3 or nonsilencing shRNA sequences (sh–) or GFP.

DMSO) for 48 hours, then lysed and subjected, as previously described (17), to SDS-PAGE and immunoblotting with one of the following Abs: 1:2,500 pan-Ras, 1:50 anti-K-Ras, 1:1,000 anti–β-tubulin, 1:1,000 anti–Gal-3, 1:10,000 anti–phospho-ERK, 1:2,000 anti-ERK, 1:750 anti-p21, and 1:500 anti-TTF-1. Immunoblots were then exposed to peroxidase-conjugated goat anti-mouse IgG, peroxidase-conjugated goat anti-rabbit IgG, or peroxidase-conjugated goat anti-rat IgG (all at 1:5,000), and protein bands were visualized using the ECL kit.

Ras-GTP assays

Lysates containing 1 mg protein were used for determination of Ras-GTP by the glutathione *S*-transferase-Ras binding domain of Raf pull-down assay, as previously described (17), followed by Western immunoblotting with Ras isoform–specific Abs as described above.

Infections and short hairpin RNAs

Viruses were produced by transient triple-transfections of HEK 293 cells using 6 μg retroviral vectors (OpenBiosystems) encoding for specific short hairpin RNA (shRNA) against Gal-3 (V2HS_133963) in combination with 3 μg pMD2G and 3 μg pCGP encoding the retroviral envelope, and the Gag and Pol proteins, respectively. As a control, we used 6 μg of no-silencing shRNA (OpenBiosystems, RHS1707) or MSCV-PIG–encoding GFP. Viruses were collected 48 hours after transfection. Two milliliters of viral supernatant containing 8 μg/mL polybrene (H9268; Sigma) were used for infections using very low-density cultured cells as indicated. Infected cells were allowed to recover and used at least 72 hours after infections for Western blotting, Ras-GTP pull-down assay as described below.

MTT

MTT solution was added to a final concentration of 0.5 mg/mL for 2 hours at 37°C, followed by DMSO. The plates were read on a micro-ELISA reader at a test wavelength of 570 nm and a reference wavelength of 630 nm.

Confocal microscopy

ARO cells (2×10^5 cells) were plated on glass coverslips and treated for 48 hours with 75 μmol/L FTS or the vehicle (control; 0.1% DMSO). After 72 hours, the cells were fixed then permeabilized with 0.5% Triton X-100. Samples were blocked with 2% bovine serum albumin and 200 μg/mL goat γ globulin for 30 minutes. Cells were labeled with 1 μg/mL anti–TTF-1, rat anti–Gal-3, or anti–pan-Ras Abs for 1 hour, and then with 1:750 goat anti-rabbit fluorescein, goat anti-rat fluorescein, or donkey anti-mouse cy3 Abs (Jackson), respectively. Each incubation was followed by three extensive washes. Staining intensity was analyzed with a Meta Zeiss LSM 510 confocal microscope. TTF-1 in the nucleus of each cell was quantified by ImageJ software.

Animal experiments

Athymic nude mice (ages 6 wk) were housed in barrier facilities on a 12-hour light/dark cycle. Food and water were supplied ad libitum. On day 0, ARO cells (5×10^6 cells in 0.1 mL PBS) were implanted s.c. just above the right femoral joint as previously described (17). After 7 days, by which time tumor volumes were 0.3 to 0.5 cm^3, mice were separated randomly into two groups (10 mice per group). Mice in one group were treated daily with oral Salirasib (100 mg/kg FTS) and in the other group with the vehicle only, and their volumes were determined as previously described (17).

Published OnlineFirst August 3, 2010; DOI: 10.1158/1535-7163.MCT-10-0262

After 25 days, the mice were killed by cervical translocation and the tumors were weighed. Tumors were then homogenized.

Statistical analysis

Student's t test was used for statistical analysis. A value of $P < 0.05$ was considered significant.

Results

Gal-3 expression in thyroid carcinoma correlates positively with high expression levels of K-Ras.GTP

Using the Ras binding domaine of Raf pull-down assay and pan-Ras Abs to determine expression levels of active Ras (Fig. 1A), we found that ARO, MRO, and NPA—all

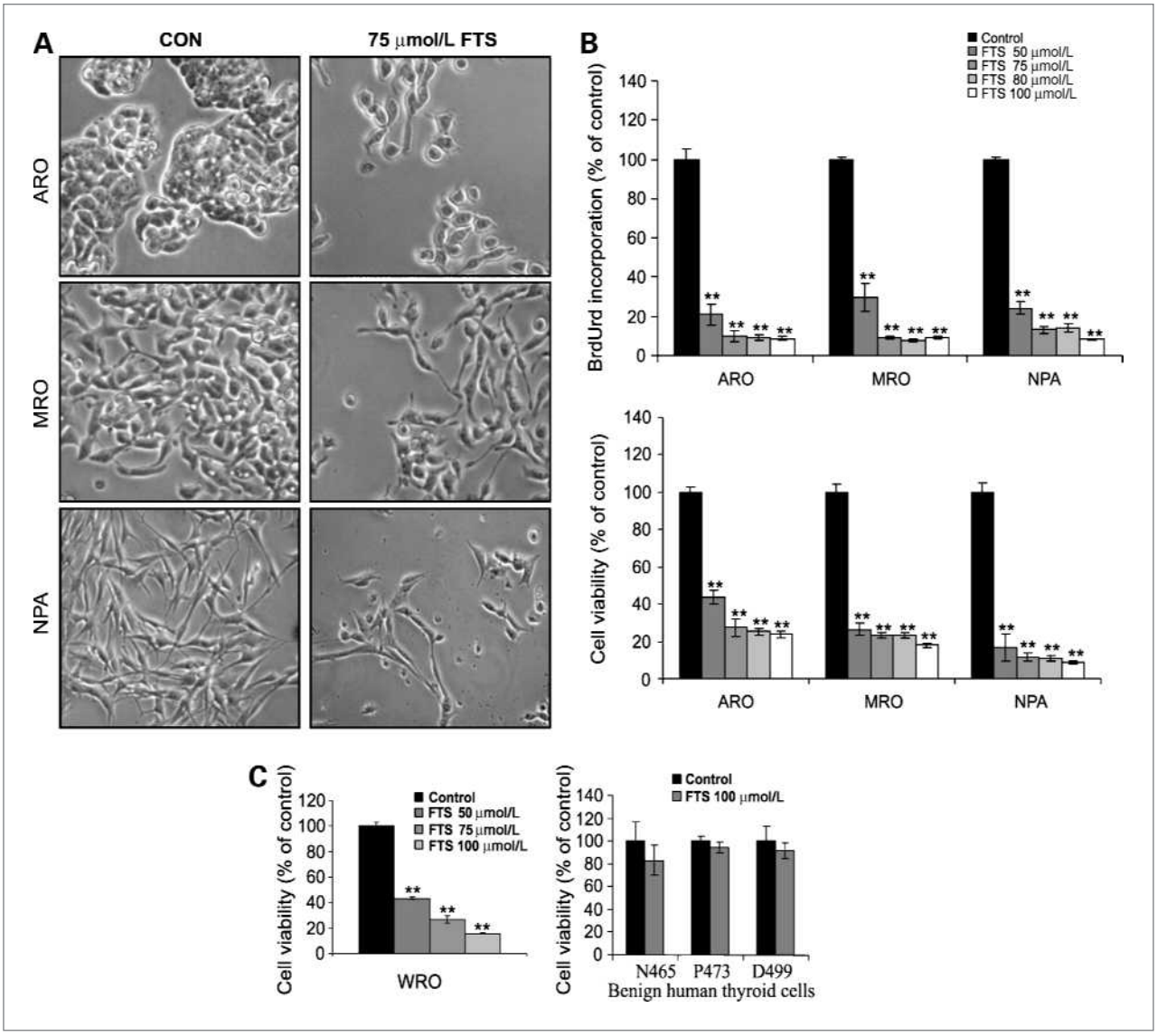

Figure 2. The Ras inhibitor FTS inhibits cell growth of thyroid carcinoma cells expressing high levels of Gal-3 protein. A, thyroid carcinoma cell growth is inhibited by FTS. Cells of the ARO, MRO, and NPA cell lines were grown (4×10^5 cells per 10-cm plate) for 48 h in the presence of 5% serum as described in Materials and Methods. They were then treated with 75 μmol/L FTS or 0.1% DMSO (vehicle control) for 72 h and visualized under a microscope. Typical phase-contrast images are shown (magnification, ×20). B, top, reduction in cell proliferation of thyroid carcinoma cells by FTS. The above cell lines (1.5×10^4 cells) were grown in the presence 5% FCS and then treated for 24 h with 50, 75, 80, or 100 μmol/L FTS or 0.1% DMSO (control). Incorporation of BrdUrd into the DNA of FTS-treated cells is expressed as a percentage of its incorporation into the control; columns, mean; bars, SEM ($n = 3$); **, $P < 0.01$. Bottom, viability of FTS-treated thyroid carcinoma cells. Cells were grown and treated as described above, and then assayed for viability using the alamarBlue reagent (see Materials and Methods). Cell viability is recorded as the amount of alamarBlue fluorescence in the FTS-treated cells expressed as a percentage of its amount in the control; columns, mean; bars, SEM ($n = 3$). C, comparison of FTS-induced reduction in cell proliferation in malignant and benign thyroid cells. WRO thyroid carcinoma cells and benign human thyroid cells N466, P473, and D499 were grown (8×10^3 cells per 24-well plate) in the presence of 5% FCS, and then treated for 72 h with FTS or 0.1% DMSO (control). Numbers of FTS-treated cells are expressed as percentages of control cell numbers. The experiment was repeated three times; columns, mean; bars, SEM. Left, results obtained for the WRO carcinoma cell line. Right, results obtained for thyroid epithelial cells from benign thyroid nodules.

Published OnlineFirst August 3, 2010; DOI: 10.1158/1535-7163.MCT-10-0262

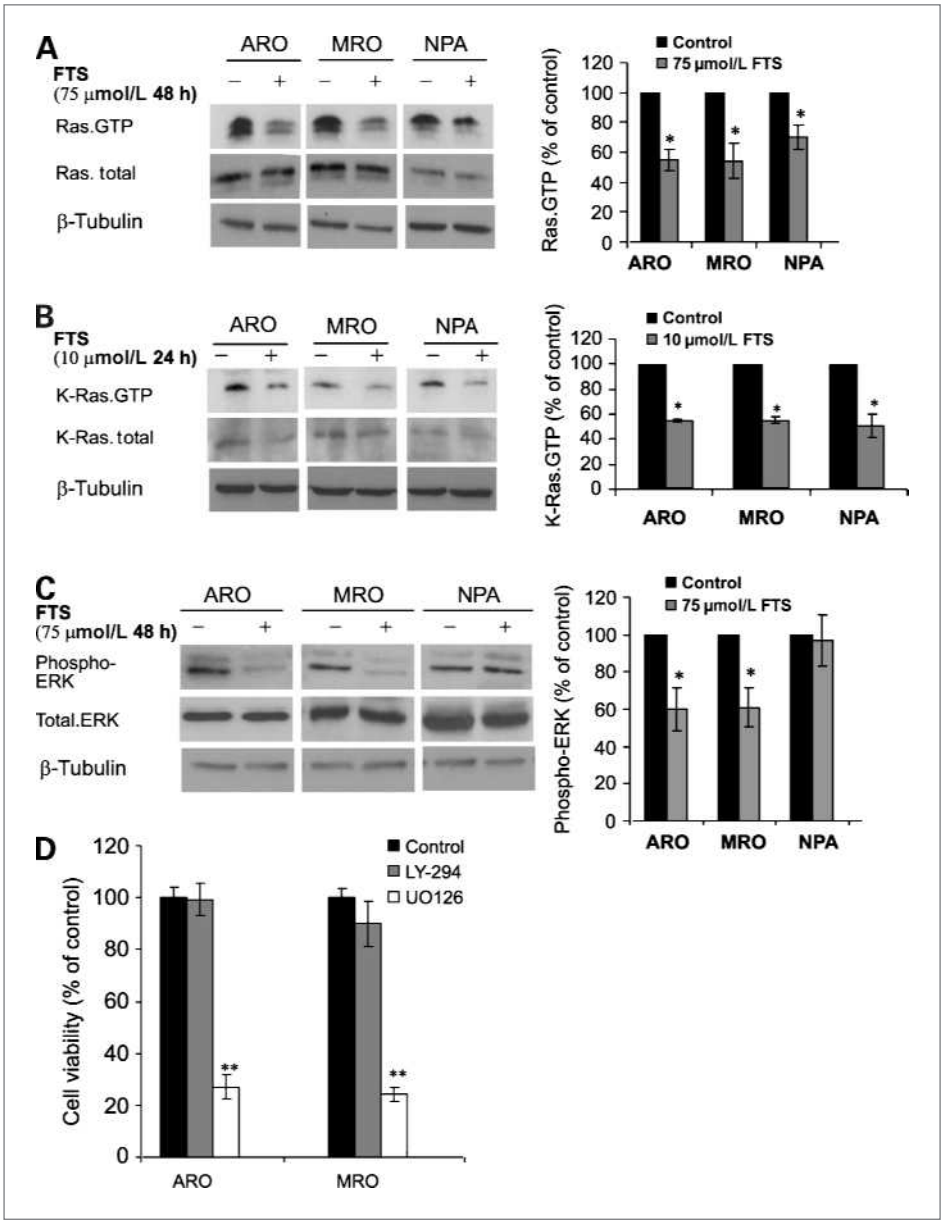

Figure 3. FTS inhibits Ras and its signals in the thyroid carcinoma ARO and MRO cells. A, FTS (75 μmol/L) reduces Ras.GTP expression in thyroid carcinoma cell lines. Cells were plated as described in Fig. 1A, treated for 48 h with 75 μmol/L FTS or vehicle (control), and then lysed. Lysates were subjected to quantification of active Ras.GTP and total Ras by SDS-PAGE, and this was followed by immunoblotting with pan-Ras Abs as described in Materials and Methods. β-Tubulin served as a loading control. Typical immunoblots visualized by ECL are shown. Immunoblots were quantified as described in Materials and Methods; right, results; columns, mean; bars, SEM ($n = 3$); *, $P < 0.05$. B, FTS (10 μmol/L) reduces K-Ras.GTP expression in thyroid carcinoma cell lines. Cells were grown as in A but at a much lower serum concentration (0.5%), treated for 24 h with FTS or vehicle (control), and then lysed. Lysates were subjected to quantification of active K-Ras.GTP and total K-Ras by SDS-PAGE and immunoblotting as described for A. β-Tubulin served as a loading control. Left, typical immunoblots visualized by ECL; right, K-Ras.GTP expression levels; columns, means; bars, SEM ($n = 3$). C, FTS (75 μmol/L) reduces phospho-ERK in ARO and MRO cells. Cells were treated as in A, lysed, and the lysates were subjected to SDS-PAGE followed by immunoblotting with anti-ERK and anti–phospho-ERK Abs. Left, typical immunoblots visualized by ECL; right, expression levels of phospho-ERK; columns, mean; bars, SEM ($n = 3$); *, $P < 0.05$. D, the MEK inhibitor UO126 but not the PI3-K inhibitor LY-294 inhibits cell growth of thyroid carcinoma. Cells of the ARO and the MRO were grown (8×10^3 cells) for 72 h in the presence of 5% serum as described in Materials and Methods. They were then treated with LY (20 μmol/L), UO126 (30 μmol/L), or 0.1% DMSO (vehicle control). Cell viability was then measured by MTT assay as described in Materials and Methods; columns, means; bars, SEM ($n = 3$); **, $P < 0.01$.

thyroid carcinoma cell lines—expressed Ras.GTP at high levels relative to the TT cell line, a thyroid carcinoma derived from the medullary rather than from the follicular epithelium, making it suitable for use as a negative control. Because none of the cell lines under study bears a Ras mutation (24, 25), the relatively high levels of Ras.GTP expression observed in these thyroid carcinomas are probably attributable to stimulation of Ras

Published OnlineFirst August 3, 2010; DOI: 10.1158/1535-7163.MCT-10-0262

exchange factors by growth factor receptors (16), and possibly also in part to the action of Ras chaperones that stabilize the active Ras.GTP (9, 17). To verify the latter possibility, we assayed Gal-3, which is known to play a role in thyroid malignancies (20, 21) and is a known chaperone of K-Ras.GTP (9, 11). We found that whereas ARO, MRO, and NPA cells expressed relatively high levels of Gal-3, the expression of this protein by the TT cells was very low (Fig. 1A). Importantly, H-Ras levels in all cell lines were so low that the levels detected with the available H-Ras–specific Ab were not significant. N-Ras expression and N-Ras.GTP could be detected, but there were no directional differences among the cell lines used (data not shown). Therefore, there is no evidence for any importance of Gal-3 expression on activation of H-Ras or N-Ras in thyroid carcinoma cells, consistent with our previous results that Gal-3 interacts only with K-Ras.GTP (9–11).

We then compared Gal-3 and active Ras expression levels in benign thyroid cells with those in malignant thyroid cells. In line with previous reports, all cell lines that were found here to express Gal-3 also expressed relatively high levels of K-Ras.GTP, whereas in the benign cells, K-Ras.GTP expression was very low, despite strong expression by these cells of the K-Ras protein itself (Fig. 1B). It should be noted that because of differences in the expression of total-ERK protein between the benign and the malignant thyroid cells, phospho-ERK expression in these experiments might be variable. Nonetheless the low levels of phospho-ERK in WRO cells (Fig. 1B) in the presence of high levels of Ras-GTP and Gal-3 might be associated with additional factors controlling ERK phosphorylation/dephosphorylation.

All in all, these results are consistent with earlier reports (9, 11, 26) that Gal-3 expression promotes high K-Ras.GTP expression, as well as signaling that allows the cells to proliferate rapidly and to exhibit marked sensitivity to the Ras inhibitor FTS. -Ras levels were so low that levels detected with the available H-Ras–specific Ab were not significant. N-Ras expression and N-Ras.GTP could be detected, but there were no directional differences among the cell line. Thus, there was no difference among cell lines in the levels of N-Ras.GTP/total N-Ras as we see in the case of K-Ras.GTP. Therefore, there is no evidence for any significance of Gal-3 on the activation of H-Ras or N-Ras, consistent with our previous results (9–11).

Finally, we performed experiments to examine if the Gal-3 phenotype thyroid carcinoma can be rescued. We found that MRO cells expressing shRNA to Gal-3 exhibited much lower levels of Gal-3, K-Ras-GTP, and phospho-ERK compared with the control (GFP or nonsilencing shRNA; Fig. 1C)

High levels of K-Ras.GTP in thyroid carcinoma cell lines correlates with inhibition of cell growth by FTS

We first examined the effects of the Ras inhibitor FTS on the growth of three types of thyroid carcinoma cells, namely the ARO (anaplastic), MRO (follicular), and NPA (papillary; refs. 24, 25) cell lines. Figure 2A shows typical photomicrographs of cells that were plated and cultured as described in Materials and Methods, and then grown for 72 hours with the addition of 75 μmol/L FTS or vehicle (control). Of all these cell lines, ARO cells exhibited the most markedly transformed phenotype and grew in clusters (Fig. 2A) consistent with their high degree of malignancy. Treatment of each of the cell lines with FTS led to a reduction in their numbers and alterations in their morphology, as well as in the cell-to-cell contacts of ARO cells and of MRO cells (Fig. 2A). The clearest effect was observed in ARO cells, which are highly sensitive to FTS treatment.

Use of the BrdUrd assay to examine the effects of the Ras inhibitor FTS on cell proliferation revealed a strong, dose-dependent inhibition of BrdUrd incorporation into the DNA of all three cell lines (Fig. 2B, top). The cell viability reagent alamarBlue indicated induction of death in all cell lines (Fig. 2B, bottom). Both the BrdUrd and the cell viability assays disclosed an IC50 of <50 μmol/L for FTS (Fig. 2B). These results are in line with early reports indicating that the higher the proliferation rate of a given tumor cell line with marked dependency on active Ras.GTP, the more sensitive the cells will be to inhibition of proliferation by FTS (27, 28).

We then compared the effect of FTS on the growth of a well-established follicular thyroid carcinoma cell line WRO (29) to its effect on the proliferation of benign thyroid cells. The malignant cells exhibited much more sensitivity than the benign cells to FTS (Fig. 2C).

FTS downregulates K-Ras.GTP and affects K-Ras signaling to ERK in the Gal-3–expressing ARO and MRO cells

On examining the effects of FTS on Ras.GTP in the various thyroid carcinoma cell lines, we found that FTS (75 μmol/L, applied for 48 h) reduced Ras.GTP expression levels while affecting total Ras only slightly (Fig. 3A). A separate experiment showed that FTS also reduced the levels of K-Ras.GTP expression (Fig. 3B). For this latter experiment, we used serum-starved cells so that the effect of FTS could be determined under basal conditions, i.e., free from any serum-related stimulatory effects. Notable are the relatively low FTS concentration used in these experiments (Fig. 3B) because they are done at low serum. Under these conditions, the free concentration of FTS is high because serum binding of the drug is avoided.

As shown in Fig. 3B, even under conditions of serum starvation, K-Ras.GTP expression was relatively high in ARO, MRO, and NPA cell lines and was reduced by FTS.

To determine whether the decrease in K-Ras.GTP expression in the FTS-treated thyroid carcinoma cells was translated into a reduction in Ras signaling, we examined phospho-ERK and phospho-Akt expression levels as readouts of the two prominent Ras pathways, Raf/MEK/ERK and PI3-K/Akt, respectively. Because phospho-Akt was not detected in any of the cell lines even in the absence of drug treatment (data not shown), it could not be used as readout

Published OnlineFirst August 3, 2010; DOI: 10.1158/1535-7163.MCT-10-0262

for Ras signaling. However, as described above (see Fig. 1), phospho-ERK was detectable in all cell lines, and treatment with FTS significantly reduced the amounts of phospho-ERK in ARO and MRO cells (Fig. 3C). In addition, the MEK inhibitor UO126 but not the PI3-K inhibitor LY-294 inhibited cell growth of thyroid carcinoma ARO and MRO (Fig. 3D). FTS, moreover, had no inhibitory effect on phospho-ERK in NPA cells (Fig. 3C). The observed

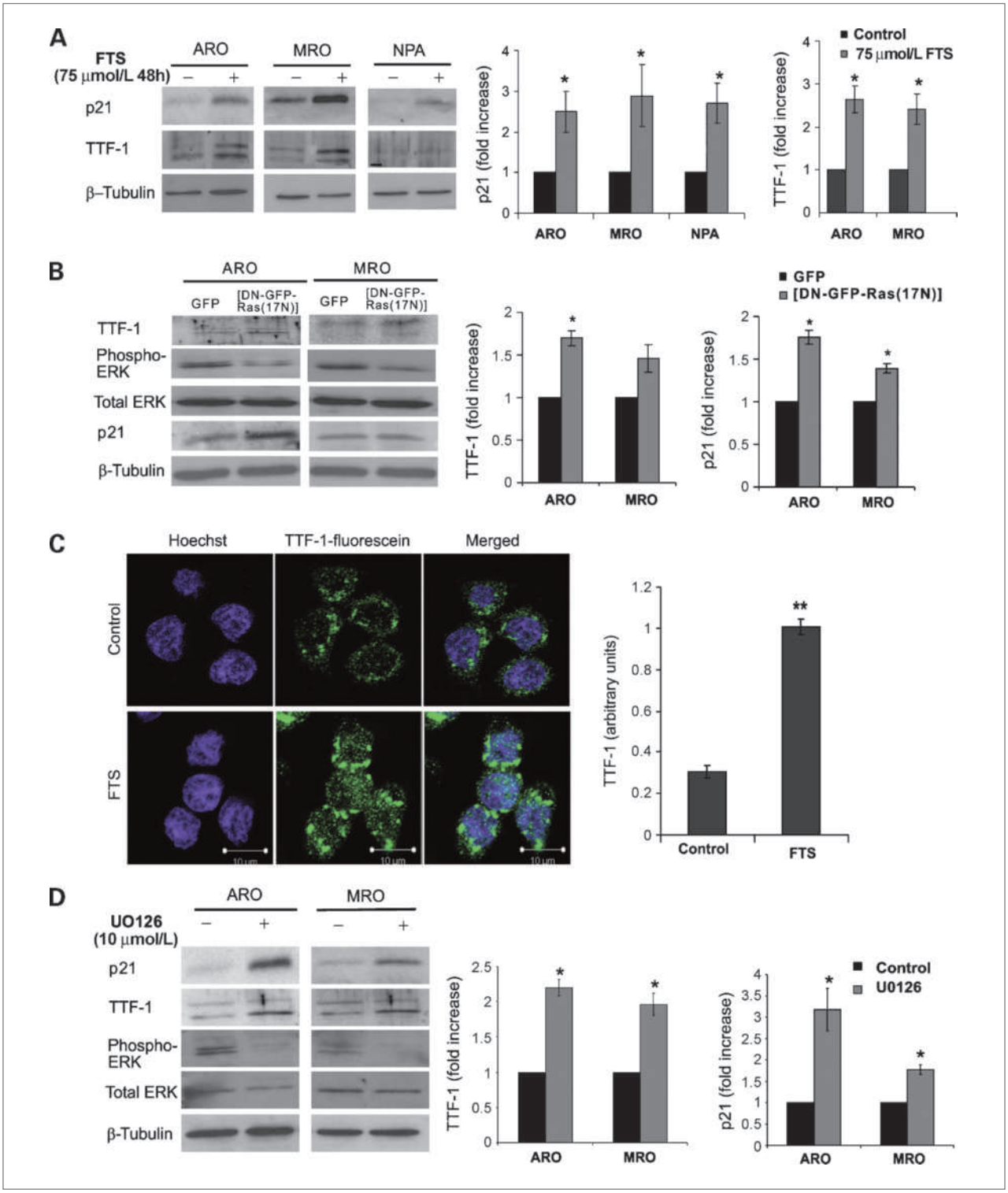

Published OnlineFirst August 3, 2010; DOI: 10.1158/1535-7163.MCT-10-0262

reduction in phospho-ERK in ARO and MRO cells, which correlated with cell growth inhibition by FTS in these two cell lines, is consistent with reports that the Raf/MEK/ERK pathway plays a critical role in thyroid carcinomas (24, 30, 31). In NPA cells, whose high K-Ras.GTP was downregulated (like that in ARO and MRO cells) by FTS (Fig. 3B), the lack of effect of FTS on phospho-ERK is probably attributable to the fact that these cells carry activating B-Raf mutations (V600E) in both alleles (32). In NPA cells, therefore, an active Ras-independent Raf signal to ERK is relatively strong. This is not the case in ARO cells, which are heterozygous with respect to the activated mutant B-Raf and carry one wild-type B-Raf allele, or in MRO cells, which carry no B-Raf mutations (24, 32). Thus, it can be expected that in ARO and MRO cell lines, the Ras-dependent activation of wild-type B-Raf will be inhibited when their K-Ras.GTP is downregulated by FTS (Fig. 3).

FTS upregulates the cell cycle inhibitor p21 and the thyroid transcription factor 1 in thyroid carcinoma cell lines

Earlier studies by our group using cancer cell lines with active Ras showed that the cell cycle inhibitor p21, which inhibits cyclin-dependent kinase 2, is negatively regulated, at least in part, by active Ras (33); accordingly, FTS was found to increase the levels of p21 expression in several cancer cell lines (34). On examining whether FTS affects p21 in the thyroid cell lines used in this study, we found that ARO, MRO, and NPA cells all exhibited an FTS-induced increase in p21 expression levels (Fig. 4A), which was accompanied by a reduction in K-Ras.GTP expression and inhibition of cell growth in these cells (Figs. 2 and 3A). Similar results were obtained with DN-Ras (Fig. 4B). It thus seems that the increase in p21 expression induced by FTS is a major factor inhibiting cell proliferation in thyroid cells that express high levels of Gal-3.

Next, we examined whether FTS affects the expression of TTF-1, which in thyroid carcinomas is negatively regulated by the Raf/MEK/ERK pathway (35). We found that TTF-1 was upregulated by FTS in ARO and MRO cells but not in NPA cells (Fig. 4A), consistently with our finding that Ras-dependent ERK activation is more sensitive to FTS in ARO and MRO cells than in the NPA cell line (Fig. 3C). Like FTS, dominant-negative (DN)-Ras downregulated phospho-ERK and upregulated both p21 and TTF-1 in ARO and MRO cells (Fig. 4B).

The above findings thus suggested that Ras inhibition by FTS or by DN-Ras reverses, at least in part, the malignant phenotype of the most malignant cell line studied here (ARO) by arresting cell growth and increasing the differentiation transcription factor TTF-1, known to be a critical factor in differentiation of thyroid cells (36). Microscopic examination of FTS-treated ARO cells indeed revealed a change in their morphology with the cells becoming more spread out and less clustered (Fig. 1A). In addition, we observed a pronounced increase in nuclear TTF-1 in these cells after FTS treatment, as well as some increase, as yet unexplained, in paranuclear TTF-1 (Fig. 4C). Like FTS, the MEK inhibitor UO126 induced a marked increase in the levels of p21 and TTF-1 expression in ARO and MRO cells (Fig. 4D), suggesting that these increases are mediated through inhibition of the Ras/Raf/MEK/ERK pathway.

Taken together, the results described above suggested that interactions of Gal-3 with K-Ras.GTP in ARO and MRO cells result in a robust signal to the Raf/MEK/ERK cascade, which negatively regulates p21 (28, 33) and TTF-1 (35, 37), and hence that K-Ras.GTP-Gal-3 complexes induce cell growth and inhibit differentiation.

FTS disrupts K-Ras-Gal-3 colocalization in cell membranes of ARO cells

The observed FTS-induced reduction in Ras.GTP, which was much stronger than the FTS effect on total Ras (Fig. 3A and B), is consistent with early reports that FTS interferes with the interactions between active Ras and the cell membrane (38, 39). It does this mostly by disrupting the Gal-3–driven nanoclustering of K-Ras.GTP and the robust signal of the nanocluster to the Raf/MEK/ERK cascade (9, 11, 26). To verify that FTS indeed

Figure 4. FTS treatment increases the carcinoma cell inhibitor p21 and thyroid transcription factor 1 in thyroid carcinoma cells. A, FTS upregulates p21 and TTF-1 expression levels in thyroid carcinoma cell lines. ARO, MRO, and NPA cells were plated and treated with 75 μmol/L FTS as described in Fig. 3A. The cells were then lysed and subjected to SDS-PAGE followed by immunoblotting with anti-p21 and anti–TTF-1 or anti-β–tubulin (control) Abs. Left, typical immunoblots visualized by ECL; right, record expression levels of p21 and TTF-1; columns, means; bars, SEM ($n = 3$); *, $P < 0.05$. Expression levels of p21 in the FTS-treated ARO, MRO, and NPA cells were significantly higher than in the corresponding controls (*, $P < 0.05$), as were TTF-1 expression levels in the FTS-treated ARO and MRO cells (*, $P \leq 0.05$). No such differences in TTF-1 expression levels were observed in the NPA cells. B, DN-Ras decreases phospho-ERK and increases TTF-1 expression in thyroid carcinoma cells. Cells were transfected with vectors expressing DN-GFP-Ras(17N) or GFP (control) as described in Materials and Methods. Cells were lysed 48 h after transfection, and the lysates were subjected to SDS-PAGE followed by immunoblotting with anti–TTF-1, anti-p21, anti–phospho-ERK, anti-ERK, and anti–β-tubulin Abs. Left, typical immunoblots from one of three experiments visualized by ECL. Right, expression levels of GFP [control and DN-GFP-Ras(17N); *, $P < 0.05$]. C, confocal fluorescence images of FTS-treated and FTS-nontreated (control) ARO cells. Cells were plated on glass coverslips and treated with FTS or vehicle (control) as described in Materials and Methods. They were then labeled with Hoechst stain and rabbit anti-TTF-1 Ab, and then with fluorescein-labeled goat anti-rabbit Ab, and imaged as described in Materials and Methods. Typical images, including dual-fluorescence merged images (green, TTF-1; blue, Hoechst-stained nuclei) are shown. Similar results were obtained in three independent experiments. Right, the relative extent of fluorescine fluorescence recorded in the expreriment [FTS treated/control; columns, mean; bars, SEM ($n = 25$ cells); **, $P < 0.01$]. D, the MEK inhibitor UO126 increases p21 and TTF-1 expression levels in ARO and MRO cells. Cells (2×10^5 cells per 6-cm plate) were grown for 24 h in RPMI containing 5% FCS with or without UO126 (10 μmol/L). Cells were lysed, and the lysates were subjected to SDS-PAGE followed by immunoblotting with anti–TTF-1, anti-p21, anti–phospho-ERK, anti-ERK, and anti–β-tubulin Abs as described in Materials and Methods. Left, typical immunoblots from one of three experiments. Immunoblots were quantified as described in Materials and Methods; right, results; columns, mean; bars, SEM ($n = 3$); *, $P < 0.05$).

Published OnlineFirst August 3, 2010; DOI: 10.1158/1535-7163.MCT-10-0262

disrupts the interaction between K-Ras and Gal-3 in the cell membrane, we used ARO cells, the most malignant of the cell lines in our series, and stained them, before and after FTS treatment, with both mouse anti-pan Ras Ab and rat anti–Gal-3 Ab. The cells were then stained with cy3-labeled anti-mouse Ab (Ras labeling, red in Fig. 5A) and with fluorescein-labeled anti-rat Ab (Gal-3 labeling, green in Fig. 5A). Typical confocal fluorescence images from these experiments showed that Ras was localized mainly to the cell membranes of the control cells (Fig. 5A, ii), and that after FTS treatment, a major fraction of Ras was mislocalized on the cytoplasm (Fig. 5A, v). It is important to note that Gal-3 in these ARO cells was found to be localized before being treated with FTS, both on the cytoplasm and on the cell membrane (Fig. 5A, i), whereas after FTS treatment most of the Gal-3 was cytoplasmic (Fig. 5A, iv). The pronounced effect of FTS on interactions between endogenous Ras and Gal-3 proteins is clearly shown in the observed disruption of Gal-3 and Ras colocalization on the plasma membrane of the drug-treated cells (Fig. 5A, iii and vi). Quantitative analysis of the results is shown in Fig. 5B. Importantly, these results show disruption of the interaction between Ras and Gal-3 in cancer cells without any exogenous expression of the two binding partners. Because we know from earlier reports that of all Ras isoforms only K-Ras.GTP interacts with Gal-3, and in view of our demonstration that expression of K-Ras.GTP levels in ARO cells is high (Fig. 1), we conclude that FTS disrupted the interaction between K-Ras.GTP and Gal-3 in the cellular plasma membranes. Our results also support the notion that FTS dislodges Ras from the plasma membrane and that the cytosolic Ras then degrades. First, we see a clear FTS-induced redistributing of K-Ras from its typical plasma membrane localization to the cytosol (Fig. 5). Second, determination of the levels of total K-Ras in the cells showed that FTS caused a reduction in the levels of the protein (Fig. 3B). These results suggest that Ras, which was dislodged from the cell membrane by FTS (Fig. 5), was then degraded.

FTS inhibits ARO cell tumor growth in a nude mouse model

To determine whether FTS can inhibit the growth of thyroid carcinomas *in vivo*, we again used ARO, the highly malignant anaplastic carcinoma cell line. This type of tumor is currently incurable. After cancer cell implantation and treatment with FTS or vehicle as described in Materials and Methods, the mice were killed for tumor weight measurement and pharmacodynamic analysis. Figure 6 presents typical results of one experiment of three that yielded similar results. Each lane represents blots obtained from one mouse (controls 1–4; FTS-treated 1–4). As shown, FTS treatment caused a significant reduction in the rate of tumor growth (Fig. 6A). Tumor weight at the end point was also significantly lower in the FTS-treated group than in the control (Fig. 6B). Figure 6C presents the results of the pharmacodynamic analysis. FTS treatment caused significant reductions in Ras.GTP, Gal-3, and phospho-ERK (Fig. 6C, i; for quantification see Fig. 6C, ii) and upregulation of TTF-1 and p21 (Fig. 6C, iii; for quantification see Fig. 6C, iv). Taken together, these results showed that FTS hits its target in the tumors *in vivo* and inhibits the growth of this anaplastic thyroid tumor.

Discussion

The results of this study showed that the Ras inhibitor FTS (Salirasib) inhibits the growth of thyroid carcinoma cells *in vitro* (Fig. 2) and the growth of thyroid tumors in

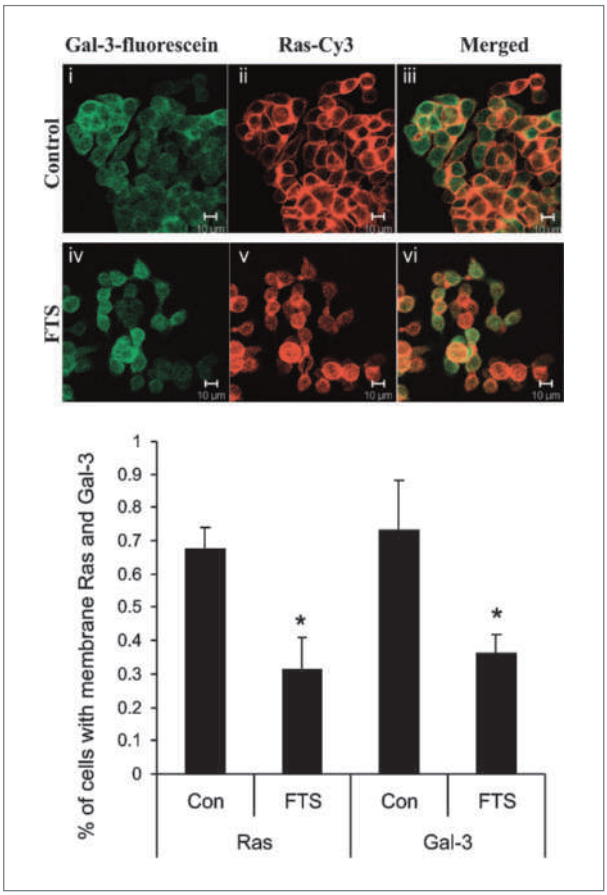

Figure 5. FTS disrupts K-Ras-Gal-3 colocalization in the cell membranes of ARO cells. ARO cells were treated with FTS or vehicle and prepared for confocal microscopy as described in Materials and Methods. Labeling with mouse anti-pan Ras Ab was followed by labeling with cy3-labeled donkey anti-mouse and rat anti–Gal-3 Abs, and then with fluorescein-labeled goat anti-rat Ab as described in Materials and Methods. A, typical dual fluorescence images (green, Gal-3; red, Ras; scale bars, 10 μm). Ras and Gal-3 are colocalized in the cell membranes of control cells. FTS treatment caused mislocalization of Ras and reduced Gal-3 in the plasma membrane. B, statistical analysis of the results. Data are presented as the numbers of cells with Ras in the plasma membrane relative to the total cell numbers and the numbers of cells with Gal-3 in the plasma membrane relative to the total cell numbers; columns, mean; bars, SEM ($n = 45$ cells); *, $P < 0.05$.

Published OnlineFirst August 3, 2010; DOI: 10.1158/1535-7163.MCT-10-0262

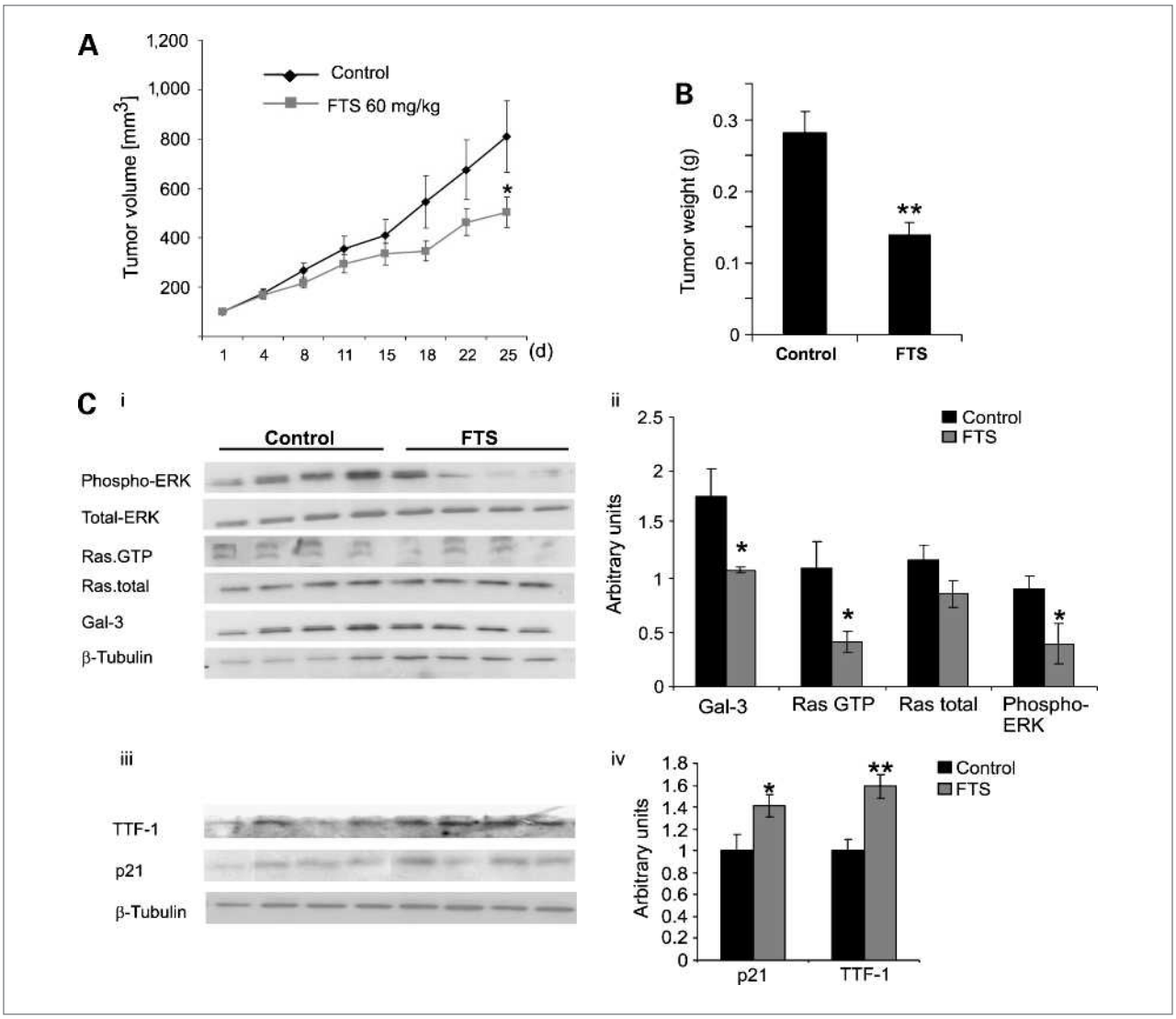

Figure 6. FTS inhibits ARO thyroid cell tumor growth in a nude mouse model. Nude mice were injected s.c. in the flank with ARO cells and treated with FTS or vehicle (control) as described in Results. Tumor volumes and weights were determined as described in Materials and Methods. A, ARO cell tumor volume in FTS-treated and control mice as a function of time; points, mean; bars, SEM; *, $P < 0.05$. B, ARO cell tumor weight on day 25 of treatment in FTS-treated and control mice; columns, mean; bas, SEM; **, $P < 0.01$. C, levels of phospho-ERK, ERK, Ras.GTP, total Ras, Gal-3, and β-tubulin in one experiment (top) and levels of TTF-1, p21, and β-tubulin in a second experiment (bottom) were determined in the tumor homogenates. Each lane represents blots obtained from one mouse (controls 1–4 and FTS treated 1–4). Left, imunoblots. Right, densitometric analysis of the results; Gal-3, Ras, Ras-GTP phospho-ERK, TTF1, and p21 expression, normalized by β-tubulin expression, in FTS-treated and control mice; columns, mean; bars, SEM ($n = 4$); *, $P < 0.05$.

a nude mouse model (Fig. 6). Consistently with the known anti-Ras activity of FTS, we showed here that FTS significantly reduced the expression levels of K-Ras.GTP and its downstream target phospho-ERK in thyroid cancer cells (Fig. 3). These findings are in accord with the mode of action of FTS, as reported in many tumor cell lines that harbor activated Ras (40, 41). Moreover, in agreement with reports that FTS can inhibit the growth of tumor cells that do not harbor *ras* gene mutations (42, 43), we found here that FTS inhibits the growth of ARO, MRO, WRO, and NPA thyroid carcinoma cell lines (Fig. 2), none of which harbors mutated Ras. The lack of correlation between *ras* gene mutations and the growth-inhibitory effects of FTS might be explained by the presence of other factors, such as hyperactive growth factor receptors that activate Ras (16, 44, 45), or the expression of Ras scaffold proteins that might lead to chronic activation of Ras (9, 17).

Here, we examined the possibility that overexpression in thyroid cancer cells of Gal-3, a selective intracellular scaffold protein of K-Ras.GTP (9, 11, 26), enhances Ras signaling and, as a consequence, may contribute to chronic activation of K-Ras. The thyroid cancer cell lines ARO, MRO, and NPA, all of which strongly express

Published OnlineFirst August 3, 2010; DOI: 10.1158/1535-7163.MCT-10-0262

Gal-3, indeed exhibited high levels of K-Ras.GTP expression when compared with TT thyroid cancer cells, in which Gal-3 expression is very low (Fig. 1). These results support our previously reported finding in a breast cancer cell line that overexpression of Gal-3 represents oncogenic subversion of K-Ras.GTP nanoclustering in the plasma membrane, thereby increasing K-Ras signal output (11, 26). In the present study, oncogenic subversion was detected in thyroid cancer cells with no exogenous expression of Ras, Gal-3, or any other oncogene or tumor suppressor. This is of particular interest because thyroid tumors that strongly express Gal-3 are extremely invasive, and their prognosis is poor (20, 21). We show here that FTS, which disrupts the interaction between K-Ras.GTP and Gal-3, induces mislocalization of both proteins from the cell membrane to the cytoplasm (Fig. 5), thereby explaining the drug-induced reduction in K-Ras.GTP. It is interesting to note that the reduction in K-Ras.GTP in ARO and in MRO was accompanied by reduction in signaling to ERK, but not to Akt, in agreement with previous reports that ERK is important and Akt less important for thyroid carcinoma growth (24, 30, 31). We also showed here that, as in many other cell lines with active Ras pathways (33, 34), FTS causes an increase in expression of the cell cycle inhibitor p21 (Fig. 4), and that this increase contributes to the attenuation of thyroid carcinoma cell proliferation in the presence of FTS.

Another important finding of this study was the pronounced stimulatory effect of FTS on the specific factor TTF-1, a major player in thyroid cell differentiation (7, 35–37). This factor is negatively regulated by the Ras/Raf/MEK/ERK cascade (35, 37), and indeed, its expression is almost completely lost in thyroid anaplastic carcinomas (46). Consistent with those reports, we found here that inhibition of the active K-Ras.GTP-Gal-3 complex by FTS was accompanied by the downregulation of phospho-ERK and upregulation of TTF-1 expression (Fig. 4). Moreover, TTF-1 was translocated to the nucleus, as would indeed be expected of a differentiation transcription factor.

Interestingly, recent studies have shown that oncogenic Ras is highly tumorigenic in thyroid cells and acts as a potent transformation factor in thyroid follicular cells (35, 37). Thus, oncogenic Ras causes growth factor–independent thyroid cell proliferation, morphologic transformation and anchorage-independent growth in thyroid cells, and thyroid tumor formation in nude mice (47–49). Moreover, in Ras-transformed thyroid cells, the expression of thyroid-specific genes is suppressed (47–50). Taken together, those findings strongly support the notion that Ras inhibition might be an effective treatment for thyroid carcinoma, particularly of Gal-3–overexpressing aggressive types. Our present results in a nude mouse model showed the feasibility of this suggestion because oral FTS reduced the expression levels of both active Ras.GTP and phospho-ERK in ARO tumors and significantly reduced tumor size. FTS (Salirasib), a nontoxic drug with minimal adverse side effects (43), may therefore be considered as a potential drug for thyroid cancer treatment.

Disclosure of Potential Conflicts of Interest

Yoel Kloog is the incumbent of The Jack H. Skirball Chair in Applied Neurobiology, Tel Aviv University.

Grant Support

Israel Science Foundation (grant no. 912/06) and by the Prajs-Drimmer Institute for the Development of Anti-degenerative Drugs (R. Levy and Y. Kloog).

The costs of publication of this article were defrayed in part by the payment of page charges. This article must therefore be hereby marked *advertisement* in accordance with 18 U.S.C. Section 1734 solely to indicate this fact.

Received 03/16/2010; revised 05/13/2010; accepted 06/14/2010; published OnlineFirst 08/03/2010.

References

1. Kondo T, Ezzat S, Asa SL. Pathogenetic mechanisms in thyroid follicular-cell neoplasia. Nat Rev Cancer 2006;6:292–306.
2. Sherman SI. Thyroid carcinoma. Lancet 2003;361:501–11.
3. Hunt JL, Tometsko M, LiVolsi VA, et al. Molecular evidence of anaplastic transformation in coexisting well-differentiated and anaplastic carcinomas of the thyroid. Am J Surg Pathol 2003;27:1559–64.
4. Sipos JA, Mazzaferri EL. The therapeutic management of differentiated thyroid cancer. Expert Opin Pharmacother 2008;9:2627–37.
5. Kebebew E, Greenspan FS, Clark OH, et al. Anaplastic thyroid carcinoma. Treatment outcome and prognostic factors. Cancer 2005;103:1330–5.
6. Ahuja S, Ernst H. Chemotherapy of thyroid carcinoma. J Endocrinol Invest 1987;10:303–10.
7. Ros P, Rossi DL, Acebron A, et al. Thyroid-specific gene expression in the multi-step process of thyroid carcinogenesis. Biochimie 1999;81:389–96.
8. Liu FT, Patterson RJ, Wang JL. Intracellular functions of galectins. Biochim Biophys Acta 2002;1572:263–73.
9. Elad-Sfadia G, Haklai R, Balan E, et al. Galectin-3 augments K-Ras activation and triggers a Ras signal that attenuates ERK but not phosphoinositide 3-kinase activity. J Biol Chem 2004;279:34922–30.
10. Shalom-Feuerstein R, Makovski V, Levy R, et al. Galectin-3 regulates RasGRP4-mediated activation of N-Ras and H-Ras. Biochim Biophys Acta 2008;1783:985–93.
11. Shalom-Feuerstein R, Plowman SJ, Rotblat B, et al. K-ras nanoclustering is subverted by overexpression of the scaffold protein galectin-3. Cancer Res 2008;68:6608–16.
12. Boriack-Sjodin PA, Margarit SM, Bar-Sagi D, et al. The structural basis of the activation of Ras by Sos. Nature 1998;394:337–43.
13. Boguski MS, McCormick F. Proteins regulating Ras and its relatives. Nature 1993;366:643–54.
14. Crul M, de Klerk G, Beijnen JH, Schellens JH. Ras biochemistry and farnesyl transferase inhibitors: a literature survey. Anticancer Drugs 2001;12:163–84.

Published OnlineFirst August 3, 2010; DOI: 10.1158/1535-7163.MCT-10-0262

15. Berrozpe G, Schaeffer J, Peinado MA, et al. Comparative analysis of mutations in the p53 and K-ras genes in pancreatic cancer. Int J Cancer 1994;58:185–91.
16. Kolibaba KS, Druker BJ. Protein tyrosine kinases and cancer. Biochim Biophys Acta 1997;1333:F217–48.
17. Elad-Sfadia G, Haklai R, Ballan E, et al. Galectin-1 augments Ras activation and diverts Ras signals to Raf-1 at the expense of phosphoinositide 3-kinase. J Biol Chem 2002;277:37169–75.
18. Santoro M, Papotti M, Chiappetta G, et al. RET activation and clinicopathologic features in poorly differentiated thyroid tumors. J Clin Endocrinol Metab 2002;87:370–9.
19. Soares P, Trovisco V, Rocha AS, et al. BRAF mutations typical of papillary thyroid carcinoma are more frequently detected in undifferentiated than in insular and insular-like poorly differentiated carcinomas. Virchows Arch 2004;444:572–6.
20. Inohara H, Honjo Y, Yoshii T, et al. Expression of galectin-3 in fine-needle aspirates as a diagnostic marker differentiating benign from malignant thyroid neoplasms. Cancer 1999;85:2475–84.
21. Saggiorato E, Aversa S, Deandreis D, et al. Galectin-3: presurgical marker of thyroid follicular epithelial cell-derived carcinomas. J Endocrinol Invest 2004;27:311–7.
22. Kraiem Z, Sadeh O, Yosef M. Iodide uptake and organification, triiodothyronine secretion, cyclic AMP accumulation and cell proliferation in an optimized system of human thyroid follicles cultured in collagen gel suspended in serum-free medium. J Endocrinol 1991; 131:499–506.
23. Kraiem Z, Sadeh O, Yosef M, et al. Mutual antagonistic interactions between the thyrotropin (adenosine 3′,5′-monophosphate) and protein kinase C/epidermal growth factor (tyrosine kinase) pathways in cell proliferation and differentiation of cultured human thyroid follicles. Endocrinology 1995;136:585–90.
24. Liu D, Liu Z, Jiang D, et al. Inhibitory effects of the mitogen-activated protein kinase kinase inhibitor CI-1040 on the proliferation and tumor growth of thyroid cancer cells with BRAF or RAS mutations. J Clin Endocrinol Metab 2007;92:4686–95.
25. Namba H, Nakashima M, Hayashi T, et al. Clinical implication of hot spot BRAF mutation, V599E, in papillary thyroid cancers. J Clin Endocrinol Metab 2003;88:4393–7.
26. Shalom-Feuerstein R, Cooks T, Raz A, et al. Galectin-3 regulates a molecular switch from N-Ras to K-Ras usage in human breast carcinoma cells. Cancer Res 2005;65:7292–300.
27. Marom M, Haklai R, Ben Baruch G, et al. Selective inhibition of Ras-dependent cell growth by farnesylthiosalisylic acid. J Biol Chem 1995;270:22263–70.
28. Blum R, Elkon R, Yaari S, et al. Gene expression signature of human cancer cell lines treated with the ras inhibitor salirasib (S-farnesylthiosalicylic acid). Cancer Res 2007;67:3320–8.
29. Estour B, Van Herle AJ, Juillard GJ, et al. Characterization of a human follicular thyroid carcinoma cell line (UCLA RO 82 W-1). Virchows Arch B Cell Pathol Incl Mol Pathol 1989;57:167–74.
30. Ouyang B, Knauf JA, Smith EP, et al. Inhibitors of Raf kinase activity block growth of thyroid cancer cells with RET/PTC or BRAF mutations *in vitro* and *in vivo*. Clin Cancer Res 2006;12:1785–93.
31. Liu D, Hu S, Hou P, et al. Suppression of BRAF/MEK/MAP kinase pathway restores expression of iodide-metabolizing genes in thyroid cells expressing the V600E BRAF mutant. Clin Cancer Res 2007;13: 1341–9.
32. Carta C, Moretti S, Passeri L, et al. Genotyping of an Italian papillary thyroid carcinoma cohort revealed high prevalence of BRAF mutations, absence of RAS mutations and allowed the detection of a new mutation of BRAF oncoprotein (BRAF(V599lns)). Clin Endocrinol (Oxf) 2006;64:105–9.
33. Halaschek-Wiener J, Wacheck V, Kloog Y, et al. Ras inhibition leads to transcriptional activation of p53 and down-regulation of Mdm2: two mechanisms that cooperatively increase p53 function in colon cancer cells. Cell Signal 2004;16:1319–27.
34. Halaschek-Wiener J, Wacheck V, Schlagbauer Wadl H, Wolff K, Kloog Y, Jansen B. A novel Ras antagonist regulates both oncogenic Ras and the tumor suppressor p53 in colon cancer cells. Mol Med 2000;6:693–704.
35. Missero C, Pirro MT, Di Lauro R. Multiple ras downstream pathways mediate functional repression of the homeobox gene product TTF-1. Mol Cell Biol 2000;20:2783–93.
36. Akagi T, Luong QT, Gui D, et al. Induction of sodium iodide symporter gene and molecular characterisation of HNF3 β/FoxA2, TTF-1 and C/EBP β in thyroid carcinoma cells. British Journal of Cancer 2008;99:781–8.
37. De Vita G, Bauer L, da Costa VM, et al. Dose-dependent inhibition of thyroid differentiation by RAS oncogenes. Mol Endocrinol 2005;19: 76–89.
38. Paz A, Haklai R, Elad-Sfadia G, et al. Galectin-1 binds oncogenic H-Ras to mediate Ras membrane anchorage and cell transformation. Oncogene 2001;20:7486–93.
39. Elad G, Paz A, Haklai R, et al. Targeting of K-Ras 4B by S-trans, *trans*-farnesyl thiosalicylic acid. Biochim Biophys Acta 1999;1452: 228–42.
40. Weisz B, Giehl K, Gana-Weisz M, et al. A new functional Ras antagonist inhibits human pancreatic tumor growth in nude mice. Oncogene 1999;18:2579–88.
41. Gana-Weisz M, Halaschek-Wiener J, Jansen B, et al. The Ras inhibitor S-trans, *trans*-farnesylthiosalicylic acid chemosensitizes human tumor cells without causing resistance. Clin Cancer Res 2002;8: 555–65.
42. Blum R, Jacob-Hirsch J, Amariglio N, et al. Ras inhibition in glioblastoma down-regulates hypoxia-inducible factor-1α, causing glycolysis shutdown and cell death. Cancer Res 2005;65:999–1006.
43. Zundelevich A, Elad-Sfadia G, Haklai R, et al. Suppression of lung cancer tumor growth in a nude mouse model by the Ras inhibitor salirasib (farnesylthiosalicylic acid). Mol Cancer Ther 2007;6:1765–73.
44. Huang HS, Nagane M, Klingbeil CK, et al. The enhanced tumorigenic activity of a mutant epidermal growth factor receptor common in human cancers is mediated by threshold levels of constitutive tyrosine phosphorylation and unattenuated signaling. J Biol Chem 1997;272: 2927–35.
45. Smith JJ, Derynck R, Korc M. Production of transforming growth factor α in human pancreatic cancer cells: evidence for a superagonist autocrine cycle. Proc Natl Acad Sci U S A 1987;84:7567–70.
46. Fabbro D, Di Loreto C, Beltrami CA, et al. Expression of thyroid-specific transcription factors TTF-1 and PAX-8 in human thyroid neoplasms. Cancer Res 1994;54:4744–9.
47. Cobellis G, Missero C, Di Lauro R. Concomitant activation of MEK-1 and Rac-1 increases the proliferative potential of thyroid epithelial cells, without affecting their differentiation. Oncogene 1998;17: 2047–57.
48. Francis-Lang H, Zannini M, De Felice M, et al. Multiple mechanisms of interference between transformation and differentiation in thyroid cells. Mol Cell Biol 1992;12:5793–800.
49. Fusco A, Berlingieri MT, Di Fiore PP, et al. One- and two-step transformations of rat thyroid epithelial cells by retroviral oncogenes. Mol Cell Biol 1987;7:3365–70.
50. Kupperman E, Wofford D, Wen W, et al. Ras inhibits thyroglobulin expression but not cyclic adenosine monophosphate-mediated signaling in Wistar rat thyrocytes. Endocrinology 1996;137:96–104.

Published OnlineFirst August 3, 2010; DOI: 10.1158/1535-7163.MCT-10-0262

Molecular Cancer Therapeutics

Galectin-3 Promotes Chronic Activation of K-Ras and Differentiation Block in Malignant Thyroid Carcinomas

Ran Levy, Meital Grafi-Cohen, Zaki Kraiem, et al.

Mol Cancer Ther Published OnlineFirst August 3, 2010.